Racemization kinetics and spin states of four-coordinate nickel(II) complexes with bidentate NS ligands, $[pyrR_2R_3(NR_1S)]_2Ni$. A comparative study

Agnete la Cour, Bibhutosh Adhikhari, Hans Toftlund*
Department of Chemistry, Odense University, DK-5230 Odense M (Denmark)

and Alan Hazell
Department of Chemistry, Aarhus University, DK-8000 Århus C (Denmark)

(Received December 23, 1991; revised July 9, 1992)

Abstract

Nine complexes of the type $[pyrR_2R_3(NR_1S)]_2Ni$ (R_1 = iPr) were synthesized in order to investigate possible relations between the spin–spin equilibrium and racemization of four-coordinate nickel(II) complexes with bidentate NS ligands. An X-ray structure analysis of bis(1,3-dimethyl-5-thiolato-pyrazol-4-isopropylaldimino-*N, S*)nickel(II) shows it to be monoclinic, space group *I2/a*, with 4 molecules in a cell of dimensions $a = 19.091(4)$, $b = 7.564(2)$, $c = 15.760(4)$ Å and $\beta = 101.818(14)°$. The structure refined to a final *R* value of 0.040 for 1144 reflections. The molecule has two-fold symmetry, the coordination at Ni is close to tetrahedral with Ni–S = 2.249(1) Å and Ni–N = 1.989(3) Å. Every complex was almost totally high spin, but small differences in spin states were found by comparisons of isotropic shifts and extinction coefficients for a pure high spin transition. The racemization was studied for three complexes by temperature dependent ^1H NMR spectroscopy. Rate constants, resulting in approximate values of $\Delta H^{\neq}$ (11.1 – 34.6 kJ/mol) and $\Delta S^{\neq}$ (−56.7 to −144 J/(K × mol)), were determined from the iPrMe shifts and linewidths. Solvent effects of the kinetics were examined for one compound: the simultaneous promotion of the low spin form and the racemization rate at low temperature in the most polar solvent indicated that the low spin form may be the racemizing species.

Introduction

Four-coordinate Ni(II) [1] will always adopt a planar configuration and a spin state $S = 0$, if it is not forced by bulky ligands into a (pseudo)tetrahedral configuration and a spin state $S = 1$ or the spin–spin equilibrium (1)

$$(S = 0) \rightleftharpoons (S = 1) \quad (1)$$

with a planar or almost planar low spin (LS) and a (pseudo)tetrahedral high spin (HS) state.

Temperature dependent ^1H NMR spectroscopy has been used in investigations of four-coordinate Ni(II) with bidentate NS or NO ligands of type **A** [2, 3].

It was found that – unless R_1 was very bulky (tBu) – the LS form in the mixture was considerable and most favoured if X = S. Thermodynamic parameters ΔH and ΔS were found, but not the exchange rate; it was so high at all temperatures that the lines derived from the LS and HS form, respectively, could not be frozen out. Just one line was observed for a proton at a position determined by the mole fractions of the two kinds of molecules.

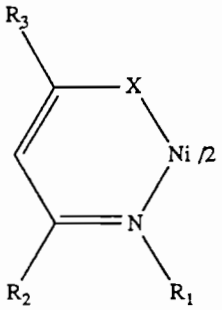

A: X = O, S

The racemization equilibrium (2) of four-coordinate

$$\Delta \rightleftharpoons \Lambda \quad (2)$$

Ni(II) with bidentate NS or NSe ligands of type **B** has been investigated by temperature dependent ^1H NMR spectroscopy [4].

*Author to whom correspondence should be addressed.

0020-1693/92/$5.00

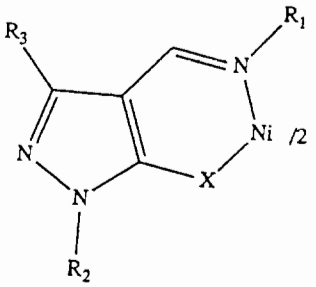

B: X = S, Se

R_1, R_2 or R_3 carries diastereotopic protons, that will change chemical shifts, when the configuration is changed in equilibrium (2). Analyses of those lines at T_c (the temperature of collapse) resulted in kinetic parameters: rate constant and $\Delta G^{\neq}$ at T_c for several compounds.

X-ray data for some type **B** complexes [5] revealed a configuration of symmetry (pseudo)D_{2d}. It was *cis*: the dihedral angle, θ, between the planes $SNiN_1$ and $N_{1a}NiS_a$ being less than 90° [6], unless R_1 was very bulky (tBu). A positive correlation was found between θ and $\Delta G^{\neq}{}_{Tc}$ supporting the proposed mechanism: a twist mechanism via a planar transition state very much like the LS form in geometry and properties [4].

The aim of this work has been to examine possible relations between the spin–spin equilibrium (1) and the racemization process (2) in a series of four-coordinate Ni(II) complexes with bidentate NS ligands.

Experimental

Nine compounds of type **B** with X = S; R_1 = iPr; R_2, R_3 = alkyl or aryl were prepared.

I: $R_2 = R_3 = Me$
II: $R_2 = Ph$, $R_3 = Me$
III: $R_2 = Me$, $R_3 = Ph$
IV: $R_2 = Me$, $R_3 = p$Cl-Ph
V: $R_2 = Me$, $R_3 = p$$NO_2$-Ph
VI: $R_2 = Me$, $R_3 = p$MeO-Ph
VII: $R_2 = R_3 = Ph$
VIII: $R_2 = Ph$, $R_3 = p$-Cl-Ph
IX: $R_2 = Ph$, $R_3 = p$MeO-Ph

Syntheses

Preparation of ligands

All ligands were prepared by the following initial steps. Condensation of the β-keto esters with the appropriate hydrazine to make the pyrazolone derivatives was followed by chloroformylation of pyrazolone (19 mmol) by phosphorous oxychloride (12.5 ml) and DMF (4.5 ml) to make the chloroaldehyde derivatives [4]. After that the following general procedure was used. The chloroaldehyde derivatives (10 mmol) in ethanol (50 ml) were stirred at room temperature with 1.0 M KSH solution (10 ml) and isopropyl amine (10 mmol) for 2 h. The mixture was heated and refluxed for 4 h followed by cooling and filtering. Excess base was neutralized by formic acid and the product concentrated. The yellow–orange ligands were finally recrystallized with a proper solvent (see Table 1).

Preparation of Ni(II) and Zn(II) complexes

General procedure. The appropriate ligand (10 mmol) was dissolved in methanol (50 ml), and Ni(II) or Zn(II) acetate (5 mmol) in methanol (25 ml) was added at room temperature. The colour immediately changed to chocolate for Ni(II) complexes and colourless or pale yellow for Zn(II) complexes. The mixture was stirred for 2 h. The product was concentrated and finally recrystallized with a proper solvent (see Table 1).

Crystal structure determination of I

Cell dimensions were determined from reflections measured at four positions, $\pm 2\theta$ and high and low χ. Intensities were measured at room temperature using a Huber diffractometer. The intensities of two standard reflections were measured every 50 reflections. (For crystal data see Table 3.)

Data were corrected for background, Lorentz and polarization effects and for absorption. The structure was determined from a Patterson synthesis and from subsequent difference electron density maps. The structure was refined by the least-squares minimization of $\Sigma w(|F_o| - |F_c|)^2$ using a modification of ORFLS [7]. All non-hydrogen atoms were refined with anisotropic thermal parameters. (Fractional atomic coordinates are listed in Table 4, bond distances and angles in Table 5.)

Susceptibility measurements of IX

Magnetic susceptibilities of the solid form of **IX** were measured according to the Faraday method. Preliminary descriptions of the instruments are found in ref. 8.

Absorption spectra

Spectra of all complexes in $CHCl_3$ and 1 cm quartz cuvettes were obtained between 200 and 2500 nm on a Shimadzu UV-3100 apparatus. Saturated solutions were used at long wavelengths, that is 3–5 mg complex per ml depending on solubility. To cover the entire range 10× dilutions were made 3–4 times. The temperature of the samples was 23.5(±0.5) °C.

^1H NMR spectra

TMS was used as internal standard in all NMR experiments. Pyrex NMR tubes were used.

Spectra of saturated solutions of all complexes in $CDCl_3$ were obtained on a Jeol JNM-PMX60SI spectrometer (60 MHz) in 5 mm tubes with a scan time of 1000 s and low filter (=5). A closed methanol standard (from Wilmad) was used for temperature calibration [9]. The temperature was 34.5(±1) °C.

TABLE 1. Solvents for recrystallization, yields and analytical data of Ni(II) and Zn(II) complexes[a]

Compound	Solvent for recrystallization	Yield (%)	Molecular formula and molecular mass	Verification	C (%)	H (%)	N (%)	S (%)	Melting point (°C)
I	MeOH	50	$C_{18}H_{28}N_6S_2Ni$	Calc.	47.92	6.21	18.64	14.20	168
	(MeOH + ether)	(60)	450.7	Found	47.82	6.22	18.66	14.25	(110)
II	MeOH + CH_2Cl_2	52	$C_{28}H_{32}N_6S_2Ni$	Calc.	58.44	5.61	14.60	11.14	230
	(EtOH + ether)	(72)	574.7	Found	58.21	5.51	14.51	11.32	(135)
III	MeOH + CH_2Cl_2	55	$C_{28}H_{32}N_6S_2Ni$	Calc.	58.44	5.61	14.60	11.14	210
	(MeOH + ether)	(68)	574.7	Found	58.09	5.71	14.55	11.21	(108)
IV	$CHCl_3$	60	$C_{28}H_{30}Cl_2N_6S_2Ni$	Calc.	52.20	4.66	13.05	9.94	196
	(EtOH)	(63)	643.7	Found	52.25	4.69	13.00	9.99	(100)
V	$CHCl_3$	65	$C_{28}H_{30}N_8O_4S_2Ni$	Calc.	50.55	4.51	16.85	9.63	> 270
	(EtOH)	(69)	664.7	Found	50.72	4.49	16.89	9.72	(210)
VI	MeOH + CH_2Cl_2	52	$C_{30}H_{36}N_6O_2S_2Ni$	Calc.	56.72	5.67	13.23	10.08	190
	(EtOH + ether)	(59)	634.7	Found	56.92	5.61	13.20	10.05	(88)
VII	$CHCl_3$	65	$C_{38}H_{36}N_6S_2Ni$	Calc.	65.24	5.19	12.01	9.17	260
	(EtOH + CH_2Cl_2)	(70)	698.7	Found	65.07	5.27	11.98	8.95	(52)
VIII	$CHCl_3$	63	$C_{38}H_{34}Cl_2N_6S_2Ni$	Calc.	59.37	4.43	10.94	8.33	250
	(EtOH + CH_2Cl_2)	(65)	767.7	Found	59.59	4.42	11.05	8.40	(95)
IX	$CHCl_3$	60	$C_{40}H_{40}N_6O_2S_2Ni$	Calc.	63.27	5.27	11.07	8.43	285
	(EtOH)	(60)	758.7	Found	63.50	5.25	11.09	8.49	(85)
III, Zn	MeOH + CH_2Cl_2	55	$C_{28}H_{32}N_6S_2Zn$	Calc.	57.80	5.50	14.45	11.00	210
			581.3	Found	57.89	5.58	14.45	11.12	
IV, Zn	MeOH + CH_2Cl_2	63	$C_{28}H_{30}Cl_2N_6S_2Zn$	Calc.	51.69	4.61	12.92	9.85	240
			651.3	Found	51.59	4.51	12.88	9.75	

[a]Data of ligands in parentheses.

TABLE 2. Chemical shifts of the Ni(II) complexes in $CDCl_3$ at 34.5 °C. Some shifts of free ligands are listed in parentheses

Compound	R_3	R_2	δ (ppm)								
			iPrMe	(iPrMe)	Me	(Me)	Ar, A	Ar, B	Ar, C	(Ar)[a]	MeO
I	Me		9.477	1.445	−13.707						
		Me			−2.840						
II	Me	Ph	9.338	1.395	−13.716	2.26	17.465	6.403	9.543	7.60	
III	Ph	Me	9.360	1.410	−1.567	3.83	7.265	5.760	7.900	7.47	
IV	*p*Cl	Me	9.509	1.425	−1.433		7.174	5.683			
V	pNO_2	Me	9.650	1.475	−0.737		7.517	6.584			
VI	*p*MeO	Me	9.292	1.405	−1.867		7.150	5.256			3.300
VII	Ph		9.051	1.420			7.580	5.900	7.917		
		Ph					17.237	6.640	9.407		
VIII	*p*Cl		9.100	1.375			7.330	5.815			
		Ph					17.190	6.614	9.350		
IX	*p*MeO		9.002	1.405			7.358	5.434			3.377
		Ph					17.237	6.656	9.348		

[a]From closely spaced lines midpoints have been chosen.

Temperature dependent spectra of a saturated solution (5 mg/ml) of **IV** in CD_2Cl_2 were obtained on a Varian EM-360 spectrometer (60 MHz) in 10 mm tubes. An external MeOH standard in 5 mm inner tubes was used for temperature calibration. MeOH was dried twice with $MgSO_4$.

Temperature dependent spectra of **II** in CD_2Cl_2 and **III** in CD_2Cl_2 and $CDCl_3$ were obtained on a Bruker AC250 spectrometer (250 MHz) in 5 mm tubes with concentrations of 1 mg/ml. The uncertainty of the temperature was 1°.

Results and discussion

Syntheses and characterization of the structure

The solvents for recrystallization, yields, and some analytical data of the complexes and ligands are given in Table 1.

Table 2 lists the chemical shifts of the Ni(II) complexes. It has not been possible with certainty to locate the positions of the isopropyl methenyl proton or the imino proton. The methenyl proton gives a paramagnetic

TABLE 3. Crystal data and details of data collection and structure refinement for **I**

FW (g mol^{-1})	451.3
Space group	$I2/a$
Cell parameters (295 K)	
a (Å)	19.091(4)
b (Å)	7.564(2)
c (Å)	15.760(4)
β	101.818(14)
V (Å^3)	2228(1)
No. reflections centred	4×30
2θ Range (°)	20.3–28.1
Calculated density (295 K) (g cm^{-3})	1.345
Molecules per cell	4
Crystal size (mm)	0.22×0.32×0.44
Developed forms	{100} {010} {001}
λ(Mo Kα) (Å)	0.71073
Monochromator	graphite
Linear absorption coefficient (cm^{-1})	10.68
Range of transmission factors	0.710–0.801
Scan type	ω–2θ
ω-Scan width	0.8+0.346 tanθ
No. steps	50
Time per step (s)	1
θ Limits (°)	1–25
Octants collected	$\pm h$ $-k$ $-l$
Standard reflections	600, 004
Fall off in intensity (%)	8
No. unique data	1929
No. data with $I/\sigma(I)>3.0$	1144
No. variables	180
Weights, w^{-1}	$[\sigma_{cs}(F^2)+1.03F^2]^{1/2}-\|F\|$
$R=\Sigma(\|F_o\|-\|F_c\|)/\Sigma\|F_o\|$	0.040
$R_w=[\Sigma w(\|F_o\|-\|F_c\|)^2/\Sigma w\|F_o\|^2]^{1/2}$	0.049
S	1.09
Δ/σ_{max}	0.08
$\Delta\rho_{max}$ (e Å^{-3})	0.19(3)

TABLE 4. Fractional atomic coordinates for **I** and equivalent isotropic thermal parameters

	x	y	z	U_{eq} (Å^2)
Ni	0.25000	0.04178(11)	0.00000	0.0590(5)
S	0.29460(6)	−0.13287(16)	−0.09156(8)	0.0686(8)
N(1)	0.3351(2)	0.1911(4)	0.0460(2)	0.052(2)
C(2)	0.3914(2)	0.2081(5)	0.0137(2)	0.050(2)
C(3)	0.4077(2)	0.1167(5)	−0.0578(2)	0.047(2)
C(4)	0.4699(2)	0.1377(6)	−0.0931(3)	0.059(3)
N(5)	0.4730(2)	0.0193(5)	−0.1531(2)	0.069(2)
N(6)	0.4133(2)	−0.0819(5)	−0.1568(2)	0.065(2)
C(7)	0.3724(2)	−0.0286(6)	−0.1015(2)	0.053(2)
C(8)	0.3380(3)	0.2920(7)	0.1294(3)	0.073(3)
C(9)	0.2709(4)	0.3888(10)	0.1289(5)	0.110(5)
C(10)	0.3588(3)	0.1697(9)	0.2038(3)	0.085(4)
C(11)	0.5260(3)	0.2769(9)	−0.0728(4)	0.085(4)
C(12)	0.4014(4)	−0.2376(10)	−0.2130(4)	0.096(5)
H(2)	0.427(2)	0.294(5)	0.041(2)	0.050(10)
H(8)	0.366(2)	0.417(7)	0.128(3)	0.101(16)
H(9A)	0.270(3)	0.464(8)	0.169(4)	0.118(21)
H(9B)	0.255(3)	0.488(6)	0.070(3)	0.106(17)
H(9C)	0.228(4)	0.271(11)	0.123(5)	0.211(36)
H(10A)	0.319(2)	0.068(7)	0.199(3)	0.097(16)
H(10B)	0.362(2)	0.228(6)	0.254(3)	0.086(16)
H(10C)	0.407(3)	0.122(8)	0.204(4)	0.143(24)
H(11A)	0.538(3)	0.301(7)	−0.010(3)	0.098(17)
H(11B)	0.569(3)	0.229(8)	−0.082(3)	0.114(19)
H(11C)	0.507(4)	0.383(9)	−0.113(5)	0.177(31)
H(12A)	0.449(4)	−0.276(9)	−0.223(4)	0.147(23)
H(12B)	0.358(3)	−0.225(7)	−0.254(3)	0.097(18)
H(12C)	0.401(5)	−0.333(11)	−0.174(5)	0.210(43)

e.s.d.s of the least significant digits in parentheses.

broadened septet; most likely it is hidden in the base noise. A signal found near 200 ppm may be due to the imino proton. The coupling constant between the iPrMe protons and the methenyl proton is not observed at any temperature because of the paramagnetic broadening of the lines. For Zn(II) analogues of **III** and **IV** it is 6.25 Hz.

Description of the crystal structure of **I**

The molecule has exact two-fold symmetry as it lies on a crystallographic two-fold axis (see Fig. 1). The coordination at the nickel atom is close to tetrahedral, the dihedral angle*, θ, between th two planes SNiN(1) and N(1′)NiS′ is 82.4(1)°. The Ni–S distance is 2.249(1) Å and Ni–N is 1.989(3) Å. These are typical values for tetrahedral NiN_2S_2 complexes and are longer than those found in the planar complexes. Values from the Cambridge Structural Database [10] are Ni–S = 2.150(3), 2.184(6) and 2.224(4) Å for *cis*, *trans* and tetrahedral complexes, and the corresponding Ni–N distances are 1.894(7), 1.921(7) and 2.002(11) Å. The S–Ni–S angle, 108.03(8)° is smaller than both the tetrahedral (109.47°) and N–Ni–N angles (110.8(2)°) suggesting a very weak attractive interaction between the sulfur atoms. The 5-thiolato-pyrazolaldimino group is planar to ±0.05 Å but the Ni atom is 0.33 Å out of this plane. The geometry of the ligand is similar to that in related compounds [11–13].

Tables 3, 4 and 5 give the X-ray data for **I**; Fig. 1 gives the three dimensional structure.

Characterization of the spin state

Magnetic measurements

Susceptibility measurements between −103 and 23 °C resulted in magnetic moments from 3.08 to 3.21 BM and thus developed a compound almost totally HS in the whole temperature range.

Absorption spectra

In four-coordinate HS Ni(II) complexes the first ligand field is found at wavelengths longer than 1000

*The dihedral angle, θ, is defined as 90° if the angle S–Ni–S is 109.47° and <90° if the S–Ni–S angle is <109.47°.

TABLE 5. Interatomic distances and bond angles for **I**

S–S′	3.639(2)
Ni–S	2.249(1)
Ni–N(1)	1.989(3)
N(1)–C(2)	1.287(5)
N(1)–C(8)	1.510(6)
C(2)–C(3)	1.410(6)
C(3)–C(4)	1.420(5)
C(4)–N(5)	1.312(5)
C(4)–C(11)	1.490(7)
N(5)–N(6)	1.363(5)
N(6)–C(7)	1.346(5)
N(6)–C(12)	1.463(7)
C(7)–S	1.717(5)
C(7)–C(30)	1.395(6)
C(8)–C(9)	1.474(8)
C(8)–C(10)	1.483(8)
S–Ni–S′	108.0(1)
S–Ni–N(1)	100.4(1)
S–Ni–N(1′)	119.2(1)
N(1)–Ni–N(1′)	110.8(2)
Ni–S–C(7)	103.7(2)
Ni–N(1)–C(2)	126.7(3)
Ni–N(1)–C(8)	119.1(3)
C(2)–N(1)–C(8)	114.2(4)
N(1)–C(2)–C(3)	127.3(4)
C(2)–C(3)–C(4)	126.7(4)
C(2)–C(3)–C(7)	128.2(4)
C(4)–C(3)–C(7)	104.6(4)
C(3)–C(4)–N(5)	111.8(4)
C(3)–C(4)–C(11)	128.1(5)
N(5)–C(4)–C(11)	120.1(4)
C(4)–N(5)–N(6)	104.7(3)
N(5)–N(6)–C(7)	113.2(4)
N(5)–N(6)–C(12)	120.3(4)
C(7)–N(6)–C(12)	126.4(5)
S–C(7)–C(3)	131.0(3)
S–C(7)–N(6)	123.3(4)
C(3)–C(7)–N(6)	105.7(4)
N(1)–C(8)–C(9)	111.6(5)
N(1)–C(8)–C(10)	109.2(5)
C(9)–C(8)–C(10)	113.9(5)

e.s.d.s. of the least significant digits in parentheses. Symmetry code: $\frac{1}{2}-x$, y, $-z$.

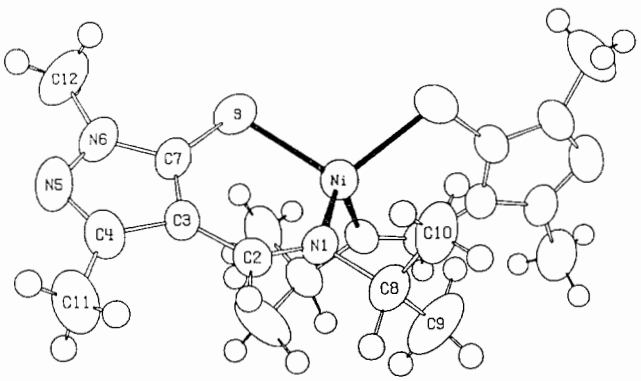

Fig. 1. The three dimensional structure of **I**.

nm. The intensity of this absorption has been used as a measure of the HS population in a spin–spin equilibrium mixture [14]. For the nine complexes the pure HS transition is between 1510 and 1575 nm (Table 6).

Differences between intensities are small. When these are plotted against the intensities of the two other transitions involving the metal centre, the d–d tranisiton at about 670 nm and the LM CT transition at about 510 nm, a slight positive correlation (about 0.5) is found. It can be ruled out that any absorption is derived mainly from LS molecules, but not that such may be present in small concentrations.

Temperature dependent ^1H NMR spectra

Table 7 lists temeprature dependent chemical shifts of **II** in CD_2Cl_2 and **III** in CD_2Cl_2 and $CDCl_3$. For **IV** in CD_2Cl_2 only the differences between the shifts of the iPrMe groups were measured at temperatures below T_c. A series of temeprature dependent spectra of **II** is shown in Fig. 2.

Plots of chemical shifts against $1/T$ resulted in straight lines (correlations close to unity) for all protons except

TABLE 6. Absorption data for the complexes in $CHCl_3$ at 23.5 °C (transitions involving metal only)

Compound	λ (nm)	ε (M^{-1} cm^{-1})	λ (nm)	ε (M^{-1} cm^{-1})	λ (nm)	ε (M^{-1} cm^{-1})
I	1575	31.3(0.6)	664	416(9.2)	505	3488(136)
II	1530	36.8(1.0)	669	493(20)	506	3618(71)
III	1575	33.6(0.7)	665	448 –[a]	508	3075 –
IV	1570	33.9(0.5)	666	422(2.0)	508	3431(74)
V	1575	34.5(0.9)	665	444(15)	509	3383(84)
VI	1575	33.1(0.7)	665	442(13)	507	3235(151)
VII	1540	32.9(0.6)	668	457(2.5)	509	3368(31)
VIII	1525	33.6(2.3)	670	463(16)	508	3185(120)
IX	1510	32.3 –	669	453(17)	509	2919(187)

s.e.s in parentheses. [a]–, measured once.

TABLE 7. Temperature dependence of the chemical shifts (for **IV** chemical shift differences between the iPrMe protons)

Compound (solvent)	T (K)	δ (ppm)					
		iPrMe(1)	iPrMe(2)	Me	Ph, A[b]	Ph, B[b]	Ph, C[b]
II	193	16.01	12.04	[a]	23.08	5.46	10.56
(CD_2Cl_2)	203	15.22	11.52	[a]	22.52	5.57	10.46
	213	14.41	10.91	[a]	21.74	5.70	10.32
	213	14.74	11.15	−22.28	21.99	5.76	10.49
	223	13.86	10.56	−20.71	21.15	5.90	10.26
	233	13.22	10.13	−19.45	20.50	6.00	10.15
	238	12.87	9.87	−18.89	20.22	6.04	10.09
	243	12.78	9.79	−18.36	19.94	6.09	10.05
	248	12.33	9.47	−17.87	19.66	6.12	9.99
	253	12.08	9.36	−17.32	19.38	6.15	9.94
	258	11.83	9.32	−16.93	19.18	6.17	9.90
	263	11.52	9.27	−16.45	18.93	6.23	9.85
	268	10.88	9.30	−16.00	18.72	6.26	9.81
	273	10.01		−15.59	18.50	6.29	9.75
	278	9.81		−15.19	18.25	6.31	9.72
	283	9.68		−14.82	18.04	6.32	9.68
	293	9.43		−14.00	17.61	6.41	9.61
	303	9.12		−13.26	17.21	6.47	9.53
III	183	16.10	12.65	−6.587	6.601	4.146	8.085
(CD_2Cl_2)	203	14.21	11.02	−5.134	6.881	4.585	8.059
	223	13.45	10.50	−4.526	6.915	4.730	7.980
	228	13.12	10.27	−4.275	6.998	4.863	8.022
	233	12.75	10.12	−4.039	7.020	4.937	8.008
	238	12.40	9.97	−3.822	7.046	5.005	7.995
	245	11.58	10.10	−3.534	7.076	5.090	7.979
	249	10.68		−3.360	7.090	5.144	7.965
	253	10.60		−3.233	7.104	5.183	7.959
	273	9.86		−2.490	7.166	5.400	7.923
	283	9.54		−2.179	7.191	5.505	7.906
	293	9.21		−1.906	7.195	5.581	7.874
III	223	14.83	11.74	[a]	6.74	4.74	7.92
($CDCl_3$)	238	13.65	11.00	[a]	6.87	4.95	7.89
	245	13.08	10.75	[a]	6.90	5.02	7.88
	249	12.95	10.90	[a]	6.94	5.09	7.88
	253	11.88		−3.50	6.96	5.13	7.87
	268	10.79		−2.94	7.03	5.30	7.84
	283	10.24		−2.45	7.09	5.44	7.83

IV (CD_2Cl_2)											
T (K)	174	175	178	181	184	188	198	202	204	215	219
$\Delta\delta$ (ppm)	5.75	5.71	5.62	5.52	5.43	5.32	5.05	4.95	4.90	4.65	4.57

[a]Signal out of phase. [b]A, B and C are the *ortho*, *meta* and *para* protons of the phenyl group.

for the chemical exchanging ones between T_{st}* and T_c. This indicated a mole fraction of HS molecules, N_{HS}, close to unity according to the equation for the temperature dependence of the isotropic contact shift (3) [15], the only one of importance for paramagnetic four-coordinate Ni(II) [16].

$$(\Delta\nu_i/\nu_o) = -A_i\gamma_e hS(S+1)N_{HS}/(3\gamma_H kT) \quad (3)$$

*T_{st} is the temperature above which chemical exchange is visible in the spectrum. As the exchange is observed first in the line shapes, T_{st} is defined here as the temperature above which broadening of lines due to exchanging protons is observed.

The dimension of the coupling constant, A_i, between the proton, i, and delocalized spin density, is in Hz. N_{HS} can be written

$$N_{HS} = n_{HS}/(n_{HS}+n_{LS}) = (1+K)^{-1} \quad (4)$$

where n is the number of moles and K the equilibrium constant for the spin–spin equilibrium (HS → LS). For $K \ll 1$ a straight line will be observed in the – normally – limited temperature range used.

Often a linear dependence of $1/T$ will be observed for the isotropic shift, but an isotropic shift different from zero will be found at infinite temperature by

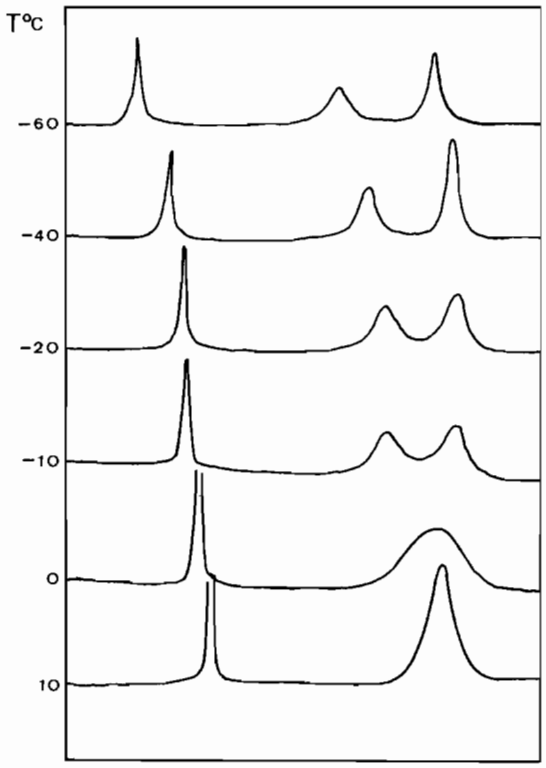

Fig. 2. Temperature dependent ^1H NMR spectra of the iPrMe group of **II** in CD_2Cl_2. The shifts of the *ortho* protons of the phenyl substituents are also shown.

extrapolation (non-Curie law dependence). An explanation may be that the complex changes slightly with temperature [17], for example by reaction with the solvent. An observed coupling constant is then not due to one complex; it is a weighted average of two or more. If the only deviation from Curie law dependence is due to spin–spin equilibrium, the observed coupling constant should be written

$$A_{i,\mathrm{obs}}(T) = A_i \times N_{\mathrm{HS}}(T) \tag{5}$$

The deviation from Curie law dependence can be included in the equation for the isotropic contact shift [18] within a relatively narrow temperature range

$$(\Delta\nu_i/\nu_o) = -A_{i,\mathrm{obs}}\gamma_e hS(S+1)/(3\gamma_H kT) + B \tag{6}$$

B may be considered an uncertainty of the coupling constant, when this is calculated from the slope of the line.

The observed coupling constants and the B values (in ppm) have been calculated for **II** and **III** (see Table 8). The correspondent free ligand has been used as the diamagnetic reference (Table 2). The deviations from Curie law dependence observed (B values, Table 8) may be due mainly to the change of N_{HS} with temperature and to chemical reaction with the solvent.

When **II** and **III** are observed in CD_2Cl_2, the solvent peak changes almost linearly with $1/T$ (Fig. 3), a sign of covalent bonding [2] between complex and solvent. TMS has been used as the internal reference, and the bulk susceptibility of the sample alone is supposed to shift all protons of the sample equally [15]. The observed shift of the solvent, then, is a weighted average of the shifts of coordinated and free solvent in fast exchange.

When **III** is observed in $CDCl_3$, the shift of the solvent is constant and equal to 7.18 ppm in the whole temperature range signifying a smaller tendency for this less polar solvent to coordinate. This same change

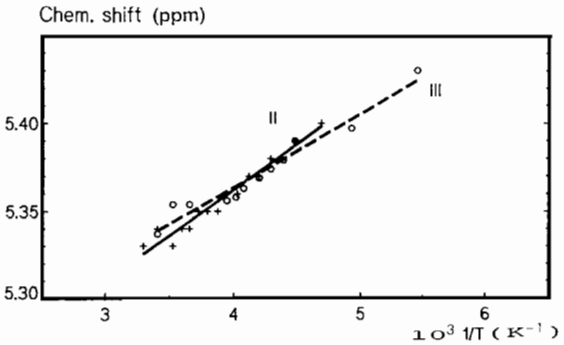

Fig. 3. From the temperature dependent ^1H NMR spectra of **II** and **III** in CD_2Cl_2; chemical shifts of the solvent plotted against $1/T$.

TABLE 8. Observed coupling constants and B values of **II** and **III** found from the direct plots of chemical shifts against $1/T$

Compound (solvent)		iPrMe(1)	iPrMe(2)	Me	Ph, A	Ph, B	Ph, C
II	B (ppm)	−1.593	−0.594	5.364	−0.868	0.639	0.056
(CD_2Cl_2)	A_i (MHz)	−0.149	−0.103	0.303	−0.152	0.025	−0.027
III	B (*ppm*)	−4.493	−5.304	1.840	0.723	0.452	0.089
(CD_2Cl_2)	A_i (MHz)	−0.166	−0.144	0.107	0.013	0.033	−0.005
III	B (ppm)			2.528	0.951	0.617	0.043
($CDCl_3$)	A_i (MHz)			0.119	0.016	0.035	−0.005

Equation (6) has been used in the following form: $\delta_{\mathrm{obs}} = -A_{i,\mathrm{obs}}\gamma_e hS(S+1)10^6/(3\gamma_H kT) + B'$; $B' = B + \delta_{\mathrm{dia}}$, B is in ppm.

of solvent gives rise to slightly increased coupling constants (Table 8) and increased isotropic shifts (Table 7).

These observations are in accordance with those made by Gerlach and Holm [3]. When comparing temperature dependent ^{1}H NMR spectra of the compound **A** (X = S) in $CDCl_3$ and CCl_4, the smallest isotropic shifts and coupling constants were found in $CDCl_3$. Further, the LS form was slightly favoured: for the process LS → HS ΔH was more positive. So was ΔS indicating the highest degree of solvation for the LS form and the strongest solvation by the most polar solvent.

It is likely that the solvation of the LS form takes place by attack from the nucleophile part of the solvent molecule, the most polar one being the best donor, on the metal centre. The complex is trapped in its almost planar LS form, that will give no contribution to the isotropic shift. Deviations from Curie law dependence will then be due mainly to the change of N_{HS} with temperature, and an observed coupling constant approximately equal to $A_i \times N_{HS}(T)$ according to eqn. (5). This is the assumption made in the discussion below.

NMR and absorption spectra

If some molecules are very similar – like the complexes investigated in this work – similar extinction coefficients and coupling constants may be expected. Different intensities of a pure HS transition and different isotropic shifts of comparable protons at a given temperature then both may express different concentrations of HS molecules. In Fig. 4 the isotropic shifts of the iPrMe protons are plotted against the extinction coefficients for the HS transition.

Almost no correlation was found, if all complexes were included (corr. = 0.2915). If **I**, the only one with no aromatic substituents on pyrazolyl, was excluded, the correlation for the remaining eight compounds increased to 0.5406. Strong correlations were found if those eight complexes were divided into two groups: (a) those with R_2 = Me and R_3 = Ar; (b) those with R_2 = Ph and R_3 = Ar, Me.

The correlations indicate that the substituent on pyrazolyl-C3 favours LS in the following direction:

(a) pNO$_2$-Ph < pCl-Ph < pH-Ph < pMeO-Ph

(b) Me < pCl-Ph < pH-Ph < pMeO-Ph

In addition, if two compounds with identical R_3s are compared, LS seems to be favoured, if R_2 is phenyl instead of methyl.

These observations are in accordance with the expected combined influence of inductive and resonance effects of metal–ligand bond strengths.

Kinetics

The temperature dependent ^{1}H NMR spectra of **II**, **III** and **IV** permitted determination of approximate values of some kinetic parameters for the racemization process of these compounds.

Rate constants were derived from the spectra of the iPrMe protons using eqns. (7) [19] and (8) [20].

$$k(T) = 0.5\pi[2(\Delta\nu_o^2 - \Delta\nu^2)]^{1/2} \quad (7)$$

$\Delta\nu_o$ is the chemical shift difference between the exchanging protons (here iPrMe) without any reduction caused by chemical exchange. In paramagnetic compounds these 'natural' chemical shift differences are seriously temperature dependent and have to be extrapolated from temperatures below T_{st} to the temperature T. $\Delta\nu$ is the observed chemical shift difference at that temperature. In Fig. 5 the $\Delta\delta$s have been plotted against $1/T$.

The conditions for use of eqn. (7) are: $\Delta\nu_o$ and $k(T) \gg \nu_{1/2}^o$. $\nu_{1/2}^o$ is the natural linewidth at half height. Like $\Delta\nu_o$ it is dependent on temperature, and has to be extrapolated to the temperature T (see below).

$$k(T) = 0.5\pi\Delta\nu_o[(\Delta\nu_o/\nu_{1/2})^2 - (\nu_{1/2}/\Delta\nu_o)^2 + 2]^{1/2} \quad (8)$$

$\nu_{1/2}$ is the linewidth at half height of the collapsed signal at the temperature T. The condition for use of eqn. (8) is: $\nu_{1/2} \gg \nu_{1/2}^o$.

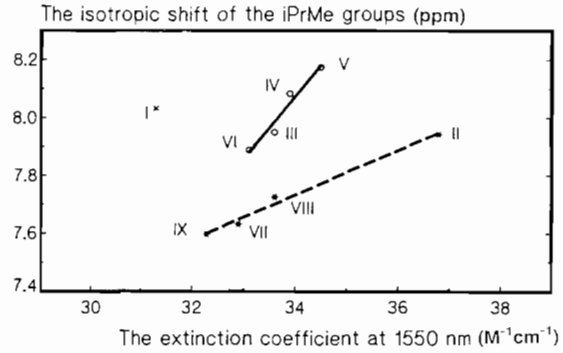

Fig. 4. The isotropic shifts of the collapsed iPrMe signal at 34.5 °C plotted against ϵ_{1550} at 23.5 °C. x: $R_2 = R_3$ = Me; o: R_2 = Me, R_3 = Ar; *: R_2 = Ph, R_3 = Ar, Me.

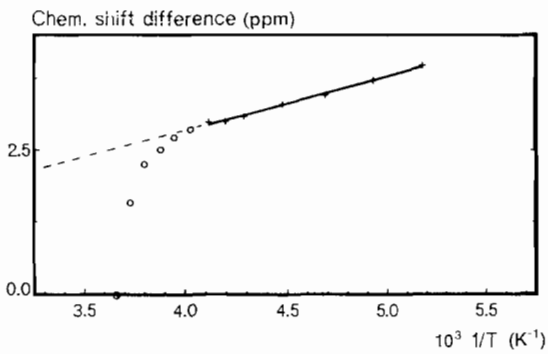

Fig. 5. The chemical shift difference between the iPrMe plotted against $1/T$. – —: Extrapolated $\Delta\delta_0$s; +, o: observed $\Delta\delta$s below and above T_{st}. (Compound **II** in CD_2Cl_2 at 250 MHz.)

TABLE 9. Temperature dependence of the linewidths in Hz (strong paramagnetic broadened lines only)

II (CD_2Cl_2)			III (CD_2Cl_2)				IV (CD_2Cl_2)		
T (K)	iPr(1)	iPr(2)	T (K)	iPr(1)	iPr(2)	Me	T (K)	iPr(1)	iPr(2)
183	499.48	231.90	183	325.18	200.11	100.05	174	102.13	83.10
193	303.26	196.23	203	220.12	150.08	75.04	175	99.72	79.77
203	267.58	178.39	223	225.12	150.08	50.03	178	93.22	79.10
213	249.74	160.55	228	250.14	175.10	45.02	181	84.75	76.27
223	200.10	[a]	233	300.16	250.14	42.52	184	79.10	70.44
233	175.09	[a]	238	[b]	[b]	37.52	219	175.14	
238	158.42	[a]	245	[b]	[b]	37.52	224	147.73	
243	208.45	125.07	249	625.30		32.52	227	135.09	
248	229.29	145.91	253	450.22		30.02	230	107.34	
253	250.13	187.60	273	162.50		30.02	237	90.40	
258	333.51	229.29	283	132.50		27.51	240	70.62	
263	416.71	354.21	293	117.50			242	67.15	
268	[b]	[b]					246	53.67	
273	583.65						272	48.02	
278	375.20						279	39.55	
283	250.13						289	33.90	
293	145.91						300	22.60	

[a]Overlap with other line. [b]Near T_c linewidths could not be measured.

Table 9 lists the measured linewidths of some strongly paramagnetic broadened lines. Plots of $\ln(\nu_{1/2}^{\circ})$ against $1/T$ resulted in correlations close to unity and showed that the temperature dependence of the natural linewidth can be fitted to eqn. (9).

$$\nu_{1/2}^{\circ}(T) = \alpha \exp(\beta/T) \tag{9}$$

As the lines from the two iPrMe were not of equal widths, $\nu_{1/2}^{\circ}{}_{av} = 1/(\pi T_{2av})$ was used for comparison, T_{2av} being the average relaxation time for the two kinds of protons calculated from the extrapolated natural linewidths.

Table 10 lists the accepted rate constants together with the $\Delta\nu_o$s, observed $\Delta\nu$s and $\nu_{1/2}$s below and above T_c, respectively, and extrapolated $\nu_{1/2}^{\circ}{}_{av}$s for comparison. As 'very much bigger than' a factor of $3\frac{1}{2} - 4$ has been accepted as a minimum.

Plots of $\ln(k/T)$ against $1/T$ resulted in correlations close to unity (-0.96 to -0.99), and $\Delta H^{\#}$ and $\Delta S^{\#}$ were found from the slope and intercept, respectively (Table 11) according to eqn. (10).

$$k(T) = T(k_B/h) \exp(\Delta S^{\#}/R) \exp[-\Delta H^{\#}/(RT)] \tag{10}$$

k_B is Bolzmann constant.

The melting point of $CDCl_3$ lies above T_{st} for **III**. As differences between spectra obtained in $CDCl_3$ and CD_2Cl_2 were in fact small, the $\Delta\nu_o$s found from the latter were used for calculations of rate constants in $CDCl_3$. The fact that T_c was higher in this less polar solvent (Table 7), indicated a slower racemization at low temperature, that is, a more positive $\Delta H^{\#}$ for the process. The kinetic parameters listed in Table 11 support this suggestion.

A possible mechanism for the racemization

Nivorozhkin *et al.* [4] found that kinetic parameters for compounds of the same type as those investigated in this work were concentration independent, and significant contributions from ligand exchange between complexes could be excluded. Kinetics are first order, and an intramolecular mechanism suggests the following possibilities:

(a) dissociation from the metal of one donor atom followed by reassociation;

(b) a twist mechanism without ligand dissociation.

Salen

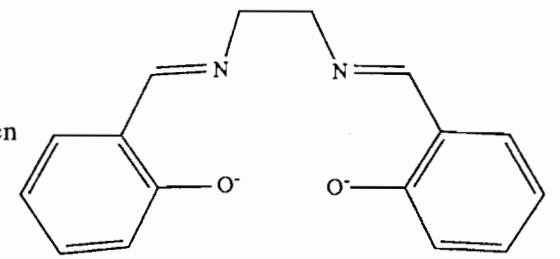

(a) seems to be a poor choice. Addition of Salen in excess to a chloroform solution of complex at room temperature resulted in slow discolouring of the solution (during several minutes) showing a half time in magnitude of minutes for reaction (11).

$$Ni(NS)_2 + Salen \rightleftharpoons NiSalen + 2(NS) \tag{11}$$

NiSalen is a very stable LS complex and Salen highly fitted to compete with bulky bidentate ligands. The rate determining step is dissociation of the first ligand [21]. The slowness of the reaction signifies a half time of (a) much longer than that of the racemization, at

TABLE 10. Rate constants calculated by eqns. (7) and (8) and checked for fulfilment of the conditions by comparison of $k(T)$ ($T \leqslant T_c$) and $\nu_{1/2}(T)$ ($T \geqslant T_c$) with extrapolated $\nu^{o}_{1/2av}$s. Extrapolated $\Delta\nu_o$s are also listed

Compound (solvent)	T (K)	$\Delta\nu_o$ (Hz)		$10^{-3} \times k$ (s^{-1})	$\nu^{o}_{1/2av}$ (Hz)
			$\Delta\nu$ (Hz)		
II	258	679.1	627.5	0.577	115.3
(CD_2Cl_2)	263	661.6	562.5	0.774	109.6
	268	644.9	395.0	1.132	104.9
	273	628.7	0.0	1.397	100.4
			$\nu_{1/2}$ (Hz)		
	273	628.7	583.65	1.497	100.4
	278	613.1	375.20	1.996	96.3
			$\Delta\nu$ (Hz)		
III	233	720.9	657.5	0.657	120.9
(CD_2Cl_2)	238	710.0	607.5	0.816	114.4
	245	695.5	370.0	1.308	106.2
	249	687.6	0.0	1.527	102.0
			$\nu_{1/2}$ (Hz)		
	249	687.6	625.30	1.667	102.0
	253	680.0	450.22	2.094	98.0
			$\Delta\nu$ (Hz)		
III	238	710.0	662.5	0.567	114.4
($CDCl_3$)	245	695.5	582.5	0.844	106.2
	249	687.6	512.5	1.018	102.0
	253	680.0	0.0	1.511	98.0
			$\nu_{1/2}$ (Hz)		
	253	680.0	667.01	1.539	98.0
			$\Delta\nu$ (Hz)		
IV	204	176.0	254.2	0.188	53.4
(CD_2Cl_2)	215	165.2	118.8	0.255	45.3
	219	161.5	0.0	0.359	42.8
			$\nu_{1/2}$ (Hz)		
	219	161.5	175.14	0.328	42.8
	224	157.1	147.73	0.370	40.0
	227	154.6	135.09	0.388	38.4

room temperature from 0.04 to 0.3 ms for **II**, **III** and **IV** (Table 11).

(b) A twist mechanism is probable, and it seems probable too that some solvents actively participate in the process by coordinating to the LS form of the complex, the more polar solvent being the most efficient. The simultaneous promotion of the LS form and the acceleration of the racemization as observed for **III** supports the following proposal for a two-step mechanism (eqn. (12)), in which both steps are rate determining.

$$\Delta_{HS} \rightleftharpoons \Delta_{LS} \rightleftharpoons \Lambda_{LS} \rightleftharpoons \Lambda_{HS} \qquad (12)$$

The LS form is here considered an intermediate with a stability defined by the equilibrium constant for the spin–spin equilibrium, and it is the LS intermediate that racemizes. A chirality is assigned to the LS form for steric reasons.

If, however, similar compounds – like **III** and **IV** – are compared in the same solvent, the results did not show that a relatively high degree of LS molecules in an equilibrium mixture will always result in the smallest $\Delta H^{\neq}$ and quickest racemization at low temperature: **III** seems to be more LS than **IV** (Fig. 4), but the smallest $\Delta H^{\neq}$ was found for **IV** (Table 11). This may be the result of a lowering of the energy for the transition state for the racemization relative to the

TABLE 11. Kinetic parameters for the racemization process for compounds **II**, **III** and **IV**

Compound (solvent)	$\Delta H^{\neq}$ (kJ/mol)	$\Delta S^{\neq}$ (J/Kmol)	$\Delta G^{\neq}(T)$ (kJ/mol) T (°C)			$10^{-3} \times k(T)$ (s^{-1}) T (°C)			$t_{1/2}$ (25 °C) (ms)
			−50	−25	25	−50	−25	25	
II (CD_2Cl_2)	34.6	−56.7	47.2	48.7	51.5	0.0393	0.287	5.78	0.12
III (CD_2Cl_2)	26.5	−75.6	43.4	45.2	49.0	0.327	1.54	15.9	0.044
III ($CDCl_3$)	30.9	−61.0	44.5	46.0	49.1	0.178	1.06	15.7	0.044
IV (CD_2Cl_2)	11.1	−144	43.2	46.8	54.0	0.361	0.736	2.19	0.32

energy of the LS form: the chloro substituted phenyl of **IV** may destabilize the LS form by inductive effects of the metal–ligand σ bonds, but stabilize a planar transition state by resonance effects relative to the unsubstituted phenyl of **III**. These results then are in accordance with the proposed mechanism.

No conclusions can be drawn from the different $\Delta H^{\neq}$s found for **II** and **III** without further investigations.

The $\Delta S^{\neq}$s are negative for the compounds examined for kinetic behaviour in accordance with the proposed mechanism. The LS form with shortened metal–ligand bonds and probably also a smaller θ will be more crowded than the HS form, and the planar configuration of the transition state even more crowded. In addition, the LS form seems to be more solvated than the HS form. For **III** the most negative $\Delta S^{\neq}$ was found in the most polar solvent (Table 11).

The differences between different compounds in the same solvent can be due only to the different positions and/or nature of the substituents on pyrazolyl. As the configurations are probably *cis*, a planar transition state is expected to be *cis* too, and a bulky R_3 will result in a more crowded transition state and a more negative $\Delta S^{\neq}$ than with a bulky R_2. This is in accordance with the $\Delta S^{\neq}$s found for **II**, **III** and **IV**.

Conclusions

Nine Ni(II) complexes with bidentate NS ligands and an isopropyl group on the donor nitrogen were synthesized, and one of these was characterized by X-ray structure analysis. The coordination geometry was found to have a *cis* (pseudo)D_{2d} symmetry.

The results indicated that the mole fraction of high spin molecules is equal to or very close to unity for every complex. However, correlations between isotropic shifts from comparable protons and the extinction coefficients from a pure high spin transition developed small differences.

For the racemization process the kinetic behaviour of three complexes was examined by temperature dependent ^1H NMR spectroscopy. For the paramagnetic complexes investigated in this work corrections were made for the temperature dependence of the isotropic contact shift and of the natural paramagnetic linewidth.

By comparison of kinetic parameters for the same compound in two different solvents a simultaneous population of the LS form and an increase in the racemization rate at low temperature was found in the most polar solvent. This indicated that the process mainly follows a route where the LS form is a necessary intermediate. Planned investigations should show if this mechanism may be generalized.

Comparisons of kinetic parameters for different complexes in the same solvent did not show that a compound containing a relatively big mole fraction of LS molecules should in general be most fitted for quick racemization at low temperature.

Acknowledgements

A.l.C. gratefully acknowledges the NMR Group, Department of Chemistry, University of Odense, especially the laboratory assistants Birthe Haack and Carsten Buch for preparing the temperature dependent NMR spectra, and the H. C. Ørsted Institute, University of Copenhagen, for the magnetic measurements. A.H. is indebted to the Carlsberg Foundation and to the Danish Research Council for the diffractometer.

References

1 G. W. Everett, Jr. and R. H. Holm, *Inorg. Chem.*, *7* (1968) 776.
2 R. H. Holm, *Acc. Chem. Res.*, *2* (1969) 307.

3 D. H. Gerlach and R. H. Holm, *J. Am. Chem. Soc., 91* (1969) 3457.
4 A. L. Nivorozhkin, M. S. Korobov, L. E. Konstantinovskii, L. E. Nivorozhkin and V. I. Minkin, *J. Gen. Chem. USSR,* (1985) 757.
5 A. L. Nivorozhkin, L. E. Nivorzhkin and V. I. Minkin, *Polyhedron, 10* (1991) 179.
6 A. L. Nivorozhkin, E. V. Sukholenko, L. E. Nivorozhkin, N. I. Borisenko and V. I. Minkin, *Polyhedron, 8* (1989) 569.
7 W. R. Busing, K. O. Martin and H. A. Levy, *ORFLS, Rep. ORNL-TM-305,* Oak Ridge National Laboratory, TN, USA, 1962.
8 E. Pedersen, *Acta Chem. Scand., 26* (1972) 333.
9 A. L. Van Geet, *Anal. Chem., 42* (1970) 679.
10 F. H. Allen, O. Kennard and R. Taylor, *Acc. Chem. Res., 16* (1983) 146.
11 O. P. Anderson, J. Becher, H. Frydendahl, L. F. Taylor and H. Toftlund, *J. Chem. Soc., Chem. Commun.,* (1986) 699.
12 T. G. Takhirov, O. A. D'yachenko, D. B. Tagiev, A. L. Nivorozhkin, L. E. Nivorozhkin and V. I. Minkin, *Koord. Khim., 14* (1988) 237.
13 A. I. Uraev, A. L. Nivorozhkin, A. S. Frenkel, A. S. Antsishkina, M. A. Porai-Koshits, L. E. Konstantinovsky, G. K.-I. Magomedov and A. D. Garnovsky, *J. Organomet. Chem., 368* (1989) 303.
14 L. H. Pignolet, W. Dew. Horrocks, Jr. and R. H. Holm, *J. Am. Chem. Soc., 92* (1970) 1855.
15 J. P. Jesson, in G. N. La Mar, W. DeW. Horrocks, Jr. and R. H. Holm (eds.), *NMR of Paramagnetic Molecules,* Academic Press, New York, 1973, Ch. 1.
16 G. N. La Mar, W. Dew. Horrocks, Jr. and L. C. Allen, *J. Chem. Phys., 41* (1964) 2126.
17 W. D. Perry and R. S. Drago, *J. Am. Chem. Soc., 93* (1971) 2183.
18 L. Que, Jr. and L. H. Pignolet, *Inorg. Chem., 12* (1973) 156.
19 H. S. Gutowsky and C. H. Holm, *J. Chem. Phys., 25* (1956) 1228.
20 A. Allerhand, H. S. Gutowsky, J. Jonas and R. A. Meinzer, *J. Am. Chem. Soc., 88* (1966) 3185.
21 M. Schumann and H. Elias, *Inorg. Chem., 24* (1985) 3187.